*Covenant Journal of Engineering Technology (CJET) Vol. 1, No. 1, March 2018*

An Open Access Journal Available Online

# Experimental Investigation of Cutting Parameters on a Turning Tool Flank Wear

(Industrial and Production Engineering)

**F. Onoroh[1], M. Ogbonnaya[1], C. B. Echeta[2]**

[1]Department of Mechanical Engineering,
University of Lagos, Akoka, Yaba, Lagos, Nigeria
[2]Department of Mechanical Engineering,
Nnamdi Azikiwe University, Awka, Anambra state, Nigeria
E-mail: onofrankus@yahoo.com Phone: +23408074648666

***Abstract-*** Tool life has been a major source of concern to manufacturers, the extent of usefulness of any tool depends on it. The major cause of tool failure is tool wear and the most important aspect of wear to a machinist is the flank wear as it is the flank that is in direct contact with the work piece. This research investigates various cutting parameters and how they contribute to tool wear. The model used is the new wear model proposed by Palmai. The research involved the experimental investigation of turning on the Sumore SP 2110 lathe machine using ISOP Tungsten Carbide and High Speed Steel (HSS) as tools and Bright Mild Steel and Stainless Steel as work piece. The experimental data were used to calibrate the Palmai model for the various cutting tool and work piece pair, at different cutting parameters of spindle speeds depth of cut and feed rate. Experimental and Paimai wear results show good correlation, with about 1.5% to 5.4% deviation.

**Keywords**: Tool life, Palmai model, Flank wear, Carbide tool, High Speed Steel.

## I. Introduction

Machining is an integral process for the production of metal products. It is the broad term used to describe removal of materials from a work piece; it covers several processes such as turning, milling**,** drilling**,** shaping**,** broaching etc**.** All these machining processes involve cutting; the removal of portions of the work piece in order to get the desired geometry and size of the prescribed component [1-4]. A cutting tool has one or more sharp cutting edges and is made of a material that is harder than the work piece material. The cutting edge serves to separate chip from the work piece material.

Connected to the cutting edge are the two surfaces of the tool namely;

A. The rake face: The rake face which directs the flow of newly formed chip is oriented at a certain angle called the rake angle. It is measured relative to the plane perpendicular to the work piece surface. The rake angle can be positive or negative.

B. The flank: The flank of the tool provides a clearance between the tool and the newly formed work piece surface, thus protecting the surface from abrasion, which would degrade the finishing. The angle between the work piece surface and the flank surface is called the relief angle.

The cutting tool cuts the work piece by direct contact; as a result friction occurs between their interfaces. This leads to wear on the flank side of the tool known as flank wear. It appears in form of so called wear land and it affects to a great extent the mechanics of cutting forces. If the amount of flank wear exceeds some critical value, excessive cutting force may cause tool failure. Usually during metal cutting, cutting tools are subjected to extremely arduous conditions, high surface loads, and high surface temperatures arise because the chip slides at high speed along the tool rake face while exerting very high normal pressures (and friction force) on this face. The forces may be fluctuating - due to the presence of hard particles in the component micro-structure, or more extremely, when interrupted cutting is being carried out. Hence cutting tools need high strength at elevated temperatures, high toughness, high wear resistance and high hardness. There are two basic types of cutting tools: Single point tool

A single point tool has one cutting edge and is used for turning, boring and planning. During machining, the point of the tool penetrates below the original work piece surface of the work part. The point is sometimes rounded to a certain radius, called the nose radius. Multiple-cutting-edge tool Multiple-cutting-edge tools have more than one cutting edge and usually achieve their motion relative to the work part by rotating. Drilling and milling uses rotating multiple cutting edge tools. Although the shapes of these tools are different from a single point tool, many elements of tool geometry are similar [5].

A key factor in the wear rate of virtually all tool materials is the temperature reached during operation, cutting conditions of spindle speed, depth of cut and feed rate, unfortunately it is difficult to establish the values of this parameters needed for such calculations, however experimental measurements have provided the basis for empirical approaches.

It is common to assume that all the energy used in cutting is converted to heat and that 80% of this is carried away in the chip. This leaves about 20% of the heat generated going into the cutting tool. Even when cutting mild steel tool temperatures can exceed $550^{o}C$, the maximum temperature high speed steel (HSS) can withstand without losing some hardness.

Turning operation is described as one of the most basic and important machining processes in which the part is rotated while a single point

cutting tool is moved parallel to the axis of rotation.

Turning can be done on the external surface of the part as well as internally. The starting material is generally a work piece generated by other processes such as casting, forging, extrusion, or drawing. During turning the cutting tool removes material from the component to achieve the required shape, dimension and surface finish. However, wear occurs during the turning process which will ultimately result in the failure of the cutting tool. When the wear reaches a certain extent, the tool or active edge has to be replaced to guarantee the desired cutting action [6, 7]. Fig. 1 shows a schematic of the turning operation.

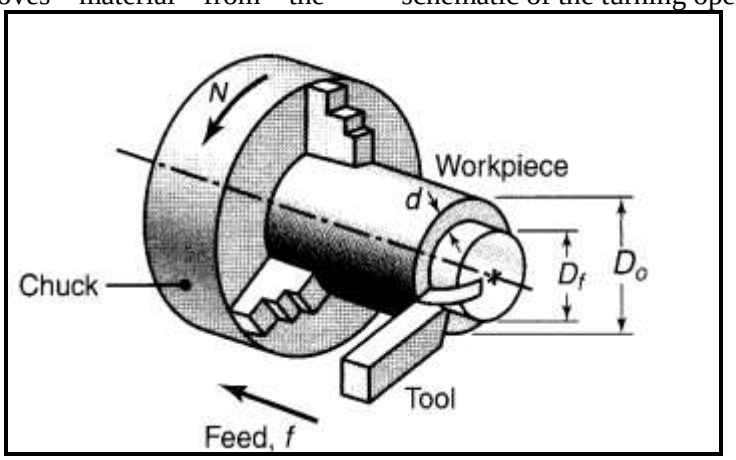


Fig. 1: Turning Operation. [8]

Limbasiya [4], in his seminar work on tool wear approached tool wear measurement using machine vision which consists of a camera, frame grabber, lighting object and processor. These components allow the system to capture the 2D representation of the object and extract the useful information from the image.


Fig. 2 Image of cutting tool [6]

From Fig. 2 it can be seen that the tool consists of three important sides: the major flank, the minor flank and the face at the top. However, the ordering of the sides is dependent on the application. Major flank is the cutting edge, while minor flank faces

the newly cut surface and the face receives the material being cut and forms chips. Tool wear can be describe as the change in shape of a tool from its original shape, during cutting, resulting from the gradual loss of tool material or deformation and the tool wear measure indicate a dimension to be measured to quantify the amount of wear.

According to the ISO standard 3685:1993, there are multiple types of wear and phenomena, which can cause tool-life criterion to be fulfilled, a tool-life criterion is a predetermined threshold value of a tool wear measure and the tool life is the cutting time required to reach a tool life criterion. Most important of the wear types are flank wear and crater wear. Flank wear is present in all situations and it is the best known type of wear. It can be found on the major flank of the tool. Fig. 3 depicts the progression
of wear as a function of time.

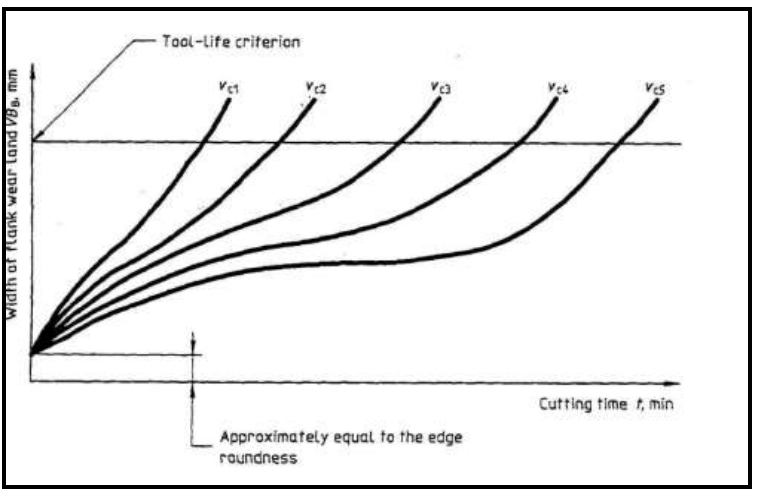


Fig. 3 Flank wear progress as a function of time [9]

Fig. 3 shows that flank wear progresses as a function of time while the general shape of the curve stays the same, cutting conditions or cutting parameters affect the tool life, i.e. the gradient of the curve, especially the linear section. Most important cutting parameters in relation to tool wear are cutting speed and feed rate, of these, cutting speed is considered to have the most effect on the tool life. The importance of cutting speed can also be seen from the Taylor's tool life equation. However there are conflicting results as feed rate has significant effect under optimal cutting temperature [10].

In order to understand the complex process of oblique cutting, the tool geometry is simplified from the three dimensional (oblique) geometry, which typifies most processes, to a two-dimensional (orthogonal) geometry. The predominant cutting action in machining involves shear deformation of the work piece to form a chip; as the chip is removed, a new surface is exposed. A typical machining process is illustrated in Fig. 4.

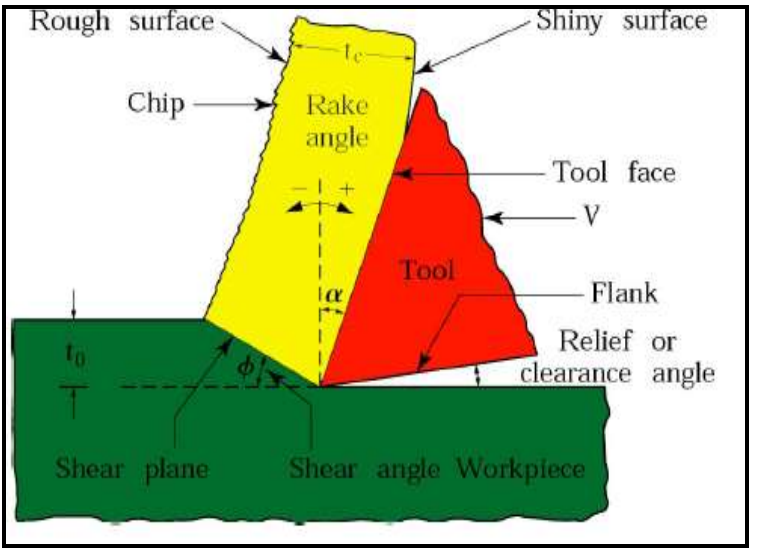


Fig. 4: Schematic illustration of a two- dimensional cutting process [11]

The flank of the tool provides a clearance between the tool and the newly generated work piece surface, thus protecting the surface from abrasion. The rake face and flank are shown in Figure 5

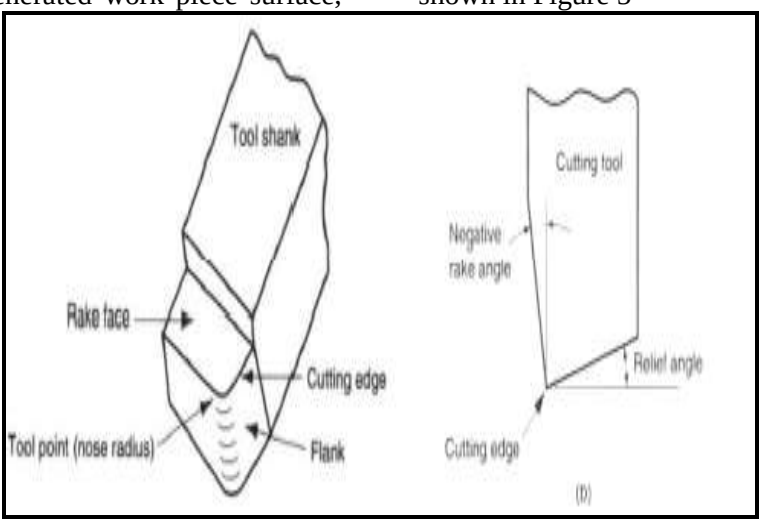


Fig. 5: A single-point tool showing rake face and flank [12]

By definition, orthogonal cutting uses a wedge shaped tool in which the cutting edge is perpendicular to the direction of cutting speed. As the tool is forced into the material, the chip is formed by shear deformation along a plane called the shear plane, which is oriented at an angle with the surface of the work piece. Only at the sharp cutting edge of the tool does failure of the material occur, resulting in separation of the chip from the work piece material. Along the shear plane, where the bulk of the mechanical energy is consumed in machining,

the material is plastically deformed. The tool in orthogonal cutting has only two elements of geometry the rake angle and the clearance angle. During cutting, the cutting edge of the tool is positioned a certain distance below the original work piece surface. This corresponds to the thickness of the chip prior to chip formation. The chip is formed along the shear plane, its thickness increases. The chip ratio can be mathematically defined as [12]:

$$r = \frac{t_0}{t_c} \quad (1)$$

Where $t_0$ , is the chip thickness prior to formation, mm, and $t_c$ is the increase in chip thickness, mm. Since the chip thickness after cutting is always greater than the corresponding thickness before cutting, the chip ratio will always be less than 1.0 In addition; the orthogonal cut has a width dimension, w, as shown in Fig. 6(a), even though this dimension does not contribute much to the analysis in orthogonal cutting. The geometry of the orthogonal cutting model allows us to establish an important relationship between the chip thickness ratio, the rake angle, and the shear plane angle as [12]:

$$t_0 = l_s \sin\varphi \quad (2)$$

And

$$t_c = l_s \cos(\varphi - \alpha) \quad (3)$$

Where $l_s$ is the length of shear plane, mm, $\alpha$ is the rake angle, grad and φ is shear plane angle, grad. Substituting equation (2) and equation (3) in equation (1) yields

$$r = \frac{l_s \sin\varphi}{l_s \cos(\varphi-\alpha)} = \frac{\sin\varphi}{\cos(\varphi-\alpha)} \quad (4)$$

This can be rearranged to determine shear plane angle, φ, as:

$$\tan\varphi = \frac{r\cos\alpha}{1 - r\sin\alpha} \quad (5)$$

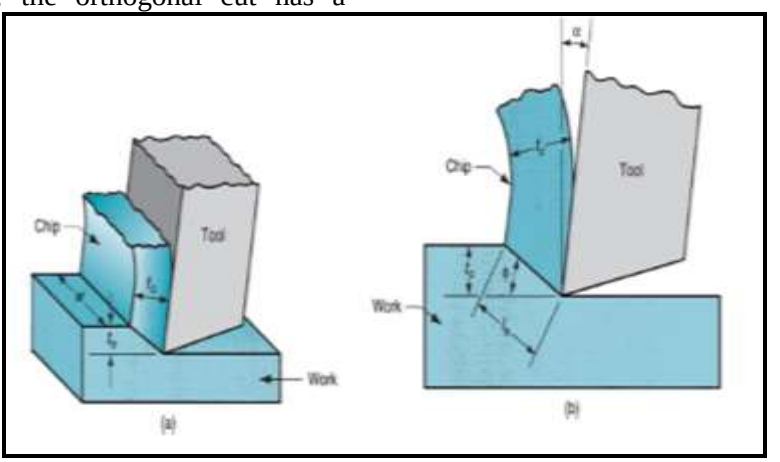


Fig. 6: Orthogonal cutting, (a) three dimension view (b) two dimensional view [12]

The shear strain that occurs along the shear plane can be estimated by examining Fig. 7. Fig. 7(a) shows shear deformation approximated by a series of parallel plates sliding against one another to form the chip. Consistent with our definition of shear strain, each plate experiences the shear strain shown in Fig. 7(b). Referring to Fig. 7(c), the shear strain can be expressed as:

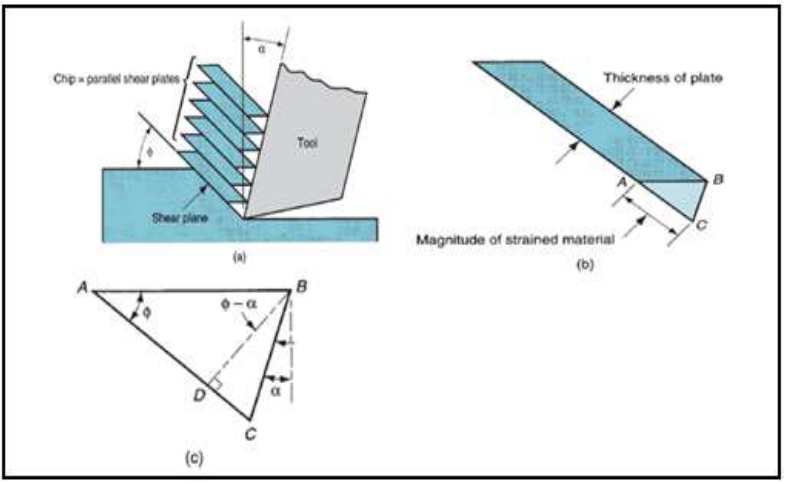

Fig. 7: shear strain during chip formation [12]

$$\gamma = \frac{AC}{BD} = \frac{AD + DC}{BD}$$

which can be reduced to the following definition of shear strain in metal cutting as:

$$\gamma = tan(\varphi - \alpha) + cot\varphi \quad (6)$$

Where $\gamma$ is the shear strain, $\varphi$ is the shear plane angle, grad and $\alpha$ is the rake angle, grad.

There are differences between the orthogonal model and an actual machining process. First, the shear deformation process does not occur along a plane, but within a zone. If shearing were to take place across a plane of zero thickness, it would imply that the shearing action must occur instantaneously as it passes through the plane, rather than over some finite (although brief) time period. For the material to behave in a realistic way, the shear deformation must occur within a thin shear zone. This more realistic model of the shear deformation process in machining is illustrated in Fig. 8.

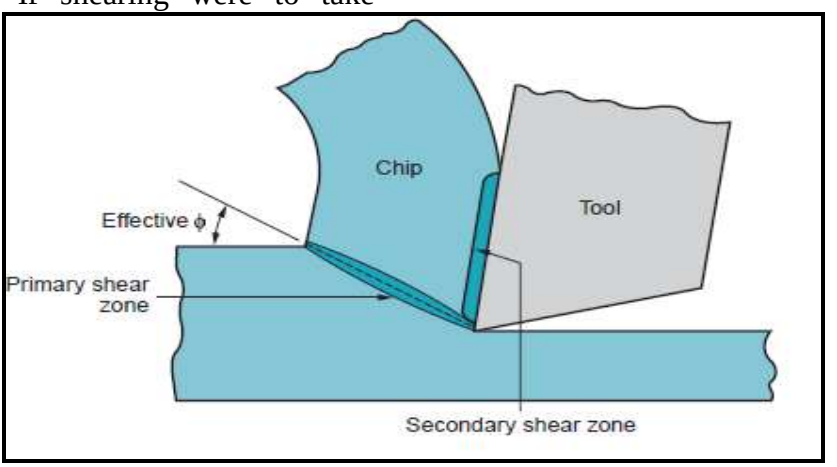

Fig. 8 Showing chip formation zone rather than the plane [12]

Metal cutting experiments have indicated that the thickness of the shear zone is only a few thousandths of an inch. Since the shear zone is so thin, there is not a great loss of accuracy in most cases by referring to it as a plane [12].

Secondly, in addition to shear deformation that occurs in the shear zone, another shearing action occurs in the chip after it has been formed. This additional shear is referred to as secondary shear to distinguish it from primary shear. Secondary shear results from friction between the chip and the tool as the chip slides along the rake face of the tool. Its effect increases with increased friction between the tool and chip. The primary and secondary shear zones can be seen in Fig. 8.

**II. Cutting Tool Flank Wear Model**

Tool wear is generally a gradual process and wear rate depends on tool and work piece materials, tool shape, cutting fluid, process parameters and machine tool characteristics. Tool wear in turn adversely affects tool life and it is one of the important criteria in determining tool life.

The most common wear of insert is flank wear. It is an abrasive wear and also can be predicted. The edge of the insert is changing its structure and the quality of work piece surface is not satisfactory. The greater the flank wear, the higher the cutting force needed for the cutting process since the insert becomes blunt at the edge of the inserts. Fig. 9 shows the sample of flank wear developed on cutting insert.

The measurement of flank wear is done from the unworn edge to the worn edge as shown in Fig. 10. The wear W measured in Fig. 10 is a failure criteria of flank wear which is 0.3 mm [14].

Fig. 9 Progression of flank wears [13]

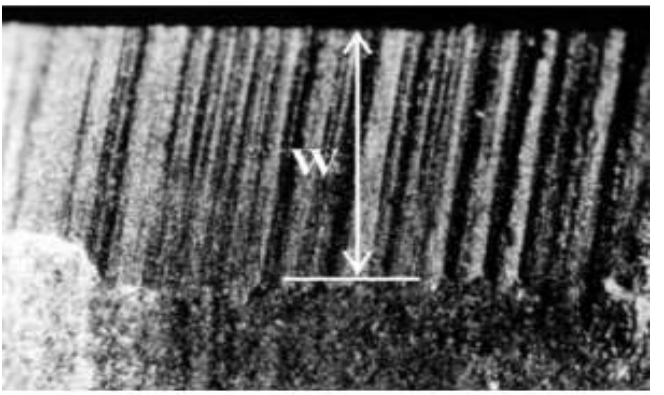


Fig. 10 Measurement of flank wear [15]

Apart from gradual tool wear, tool fracture or excessive chipping and surface roughness also affect tool life. A generalized flank wear model, crater wear model and notch wear model based on Taylor's tool life equation are used to analyze machining test results [16]. The constants in these models are found out using multiple regression analysis with the wear data collected during machining at various cutting speeds and cutting time. The wear models are:

Flank wear model

$$V_B = a_1 v^{b_1} t^{c_1} \quad (7)$$

Crater wear model

$$K_T = a_2 v^{b_2} t^{c_2} \quad (8)$$

Notch wear model

$$V_N = a_3 v^{b_3} t^{c_3} \quad (9)$$

where $V_B$, $K_T$ and $V_N$ denote flank wear, crater wear and notch wear respectively, v denotes cutting speed, m/min, t denotes machining time in minutes and $a_1$, $b_1$, $c_1 a_2$, $b_2$, $c_2$, $a_3$, $b_3$, and $c_3$ are constants.

**Geometrical Relationships of Flank Wear**

Wear can be studied in two dimensions in orthogonal cutting. The mass which is worn-off shown in Figure 11 is expressed as

$$m = \rho V \quad (10)$$

Where $\rho$ is the density and V is the volume of the worn out tool material. The volume is expressed as

$$V = (F_1 + F_2)\, b \quad (11)$$

where $F_1$ and $F_2$ are surface wear profiles and b is the width.

$F_2$ depends on the diameter of the work piece and the approach angle of the tool's edge, although it is usually ignored. The geometrical relationship of wear, using the above simplification, is shown by figure 11. The relationship between wear of x radial direction and flank wear W measured on the tool is [15]

$$W = (cot\alpha - tan\,\gamma)x \quad (12)$$

Tool flank wear is characterized by the flank wear land, VB, but the physically measurable wear parameter is the wear width, W. The geometrical relationship the two is obtained as [15]:

$$VB = \frac{W}{1 - tanatan\gamma} \quad (13)$$

The product, $tanatan\gamma \ll 1$, hence it can reasonably be assumed that, $VB = W$.

The volume, dV, worn away during time, dt, is

$$dV = bWdx \quad (14)$$

Substituting equation (12) into equation (14)

$$dV = b(cot\alpha - tan\gamma)xdx \quad (15)$$

From equation (12)

$$dW = (cot\alpha - tan\gamma)dx \quad (16)$$

From equation (12) and equation (16), equation (15) can be expressed as:

$$dV = \frac{bWdW}{cot\alpha - tan\gamma} \quad (17)$$

the volume wear rate becomes:

$$\dot{V} = \frac{b}{\cot\alpha - \tan\gamma} \times W\dot{W} \quad (18)$$

Where W is wear, $\alpha$ is rake angle, $\gamma$ shear stain rate.

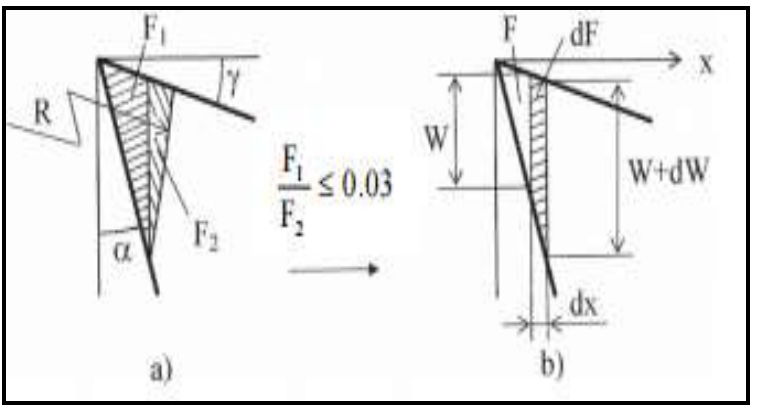


Fig. 11 The geometry of flank wears [17]

Based on the results of the morphological examinations and cutting experiments conducted on the worn surface of cutting tools it is concluded that the rate of flank wear must be studied as a function of both cutting distance and the developing temperature [17, 18].

$$\frac{dm}{dL} = \frac{\rho}{v_c}\frac{dV}{dt} = C_1 + C_2 exp\left(-\frac{Q}{R\theta(W)}\right) \quad (19)$$

Where $C_1$ and $C_2$ are assumed constants that depend on the hardness of the tool and the normal stress developed on the tool flank. The right side of equation (19) describes the physical process of wear by summarizing the adhesive/abrasive and thermally activation process, diffusion and oxidation occurring on the surface layer of the tool.

To describe the relationship between wear and temperature, equation (20) can be employed

$$\theta(W) = \theta_0 + f(W) \quad (20)$$

The new mathematical model of flank wear from the volume wear rate is obtained as:

$$\frac{dm}{dt} = \frac{v_c}{W}\left[A_\alpha + A_{th}\exp\left(-\frac{Q}{R\,[\theta_o + f(W)]}\right)\right] \quad (21)$$

where $A_\alpha$ in μm, $A_{th}$ in μm and Q in kJ/mol are constants, f is feed rate, mm/rev, m is mass in g, L is length in mm, V is volume in $mm^3$, $\theta_0$ is cutting temperature in K, $v_c$ is cutting speed in m/s, $dt$ is time interval in minutes, $R$ is general gas constant in kJ/kmolK.

The abrasive and or adhesive wear constant is obtained as:

$$A_\alpha = \frac{\cot\alpha - \tan\gamma}{b\rho} C_1 \quad (22)$$

And the thermally activated wear constant is obtained as:

$$A_{th} = \frac{\cot\alpha - \tan\gamma}{b\rho} C_2 \quad (23)$$

The temperature function of equation (20) has two parts for which the first part is mainly dependent on the technological parameters especially

the cutting speed and can be expressed as [10]:

$$\theta_0 = C_v V_c \chi \quad (24)$$

The constant $C_v$ is the cutting temperature constant, K. The second part captures the effect of wear on the tool flank temperature. The linear relationship is normally adopted as:

$$f(W) = C_w W \quad (25)$$

The constant $C_w$ is the cutting temperature wear constant,K/µm. Substituting equation (24) and equation (25) into equation (21) and designation $\frac{Q}{RC_v}$ and $\frac{C_w}{C_v}$ as B and K respectively yields:

$$W = \frac{v_c}{w}\left[A_a + A_{th}\exp\left(-\frac{B}{v_c\chi + KW}\right)\right] \quad (26)$$

The values of $C_v$, $C_w$ and χ used for steel/carbide pair are 281.5K, 0.6K/µm and 0.27 respectively [15]. Equation (26) is an autonomous non-linear differential equation which can readily be solved numerically.

## III. Experimental Method

Turning operation was carried out on both Stainless Steel and Bright Mild Steel work pieces using Carbide and High Speed Steel tool. This was carried out at different cutting parameters of cutting speed, feed rate and depth of cut. Infrared thermometer was used to record the temperature of the cutting tool and the digital weighing scale was used to determine the weight loss under these different cutting conditions after every five minutes. The measured experimental data were used to calibrate the flank wear model. Fig. 12 shows the experimental setup consisting of Carbide tool on Stainless Steel work piece undergoing turning on the Sumore SP 2110 lathe machine.

The experiment was conducted at the University of Lagos Center Research laboratory. Fig. 13 shows the Shidmazu UW 1020H digital weighing balance used to take measurement of the tool wear.

While figure 14 is the CA 879 infrared thermometer for taking temperature data

Fig. 12 High speed steel on stainless steel

Fig. 13 Shidmazu UW 1020H digital weighing scale

Fig. 14: CA 879 Infrared Thermometer

## IV. Results and Discussion

### Comparison of Experimental and Palmai wear for Carbide Tool on Bright Mild Steel at a Spindle Speed of 75 rpm

Fig. 15 shows the graph of experimental and Palmai wear against time for carbide cutting tool on bright mild steel material at a feed rate of 9.6mm/rev, spindle speed of 75rpm and depth of cut of 1mm.

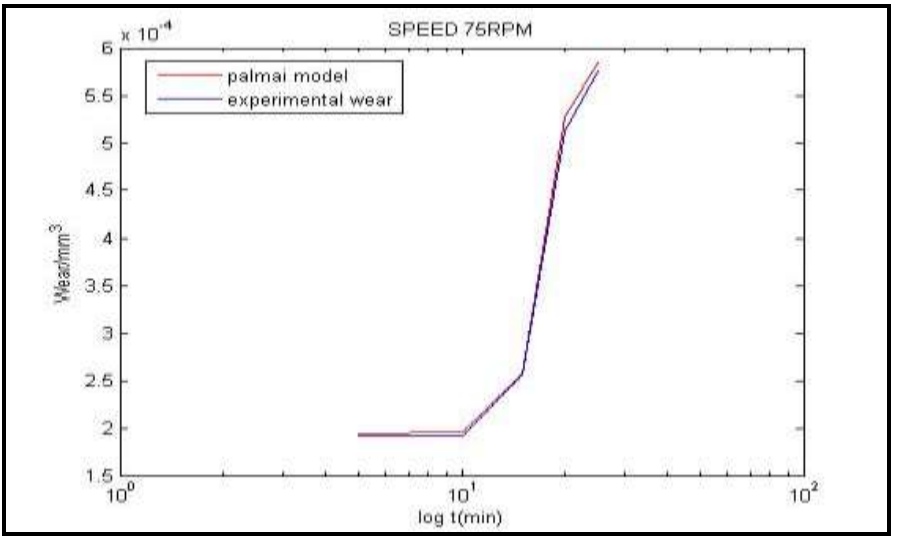

Fig. 15 Experimental and Palmai wear for Carbide Tool on Bright Mild Steel (75rpm)

The Palmai model wear constants were calibrated using the experimental data for the carbide tool bright mild steel pair. From Fig. 15 the flank wears and experimental wear data clearly increases with cutting time. Both curves are in perfect correlation as can be seen in the wear profiles. Thus the experimental wear data clearly validates the Palmai flank wear model for this tool and work piece combination.

**Comparison of Experimental and Palmai Wear for Carbide Tool on Bright Mild Steel at a Spindle Speed of 200 rpm**

Figure 16 shows the graph of experimental and Palmai wear against time for carbide cutting tool on bright mild steel material at a feed rate of 25.3rev/mm, spindle speed of 200rpm and depth of cut of 1mm.

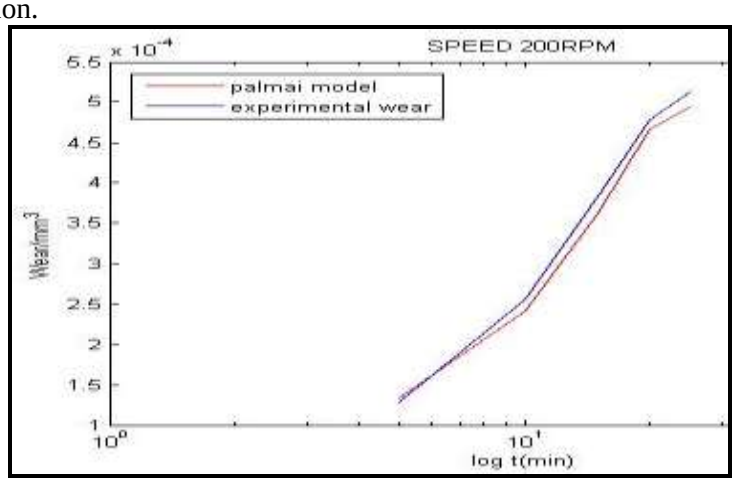

Fig. 16 Experimental and Palmai wear for Carbide Tool on Bright Mild Steel (200rpm)

The Palmai model constants were calibrated using the experimental data for the carbide tool bright mild steel pair. From Fig. 16 the flank wear and

experimental wear data clearly increases with cutting time. Both curves are in perfect correlation as can be seen in the wear profiles. Thus the experimental wear data clearly validates the palmai flank wear model for this tool/ workpiece combination.
From Fig. 15 and Fig. 16, it can be seen that flank wear increases with an increase in spindle speed.

**Comparison of Experimental and Palmai wear for Carbide Tool on Stainless Steel at a Spindle Speed of 200rpm**

Fig. 17 shows the graph of experimental and Palmai wearl against time for carbide cutting tool on bright mild steel material at feed rate of 21mm/rev, spindle speed of 200rpm and depth of cut of 2mm.

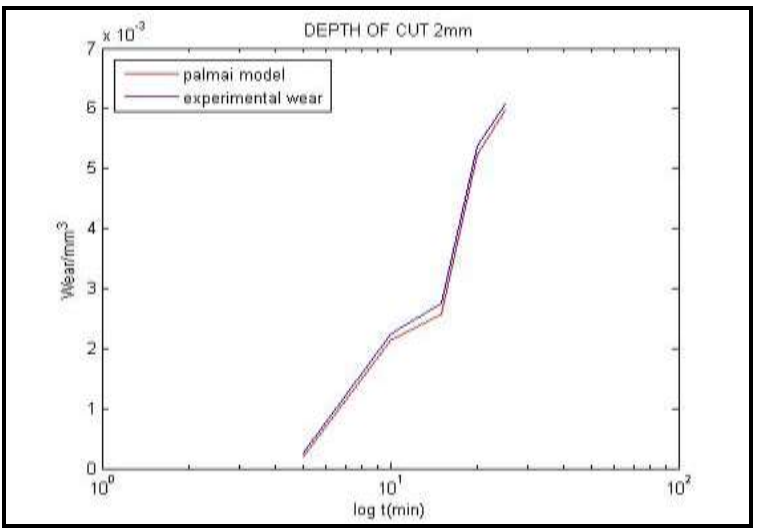


Fig. 17 Experimental and Palmai wear for Carbide Tool on Stainless Steel at 200rpm at 2mm depth of cut

The Palmai model constants were calibrated using the experimental data for the carbide tool and stainless steel pair. From Fig. 17 the flank wear and experimental wear data clearly increases with cutting time. Both curves are in perfect correlation as can be seen in the wear profiles. Thus the experimental wear data clearly validates the Palmai flank wear model for this tool and work piece combination.

**Comparison of Experimental and Palmai wear for High Speed Tool Steel on Bright Mild Steel**

Figure 18 shows the graph of experimental and Palmai wear against time for high speed steel cutting tool on bright mild steel material at feed rate of 9mm/rev, spindle speed of 75rpm and depth of cut of 1mm.

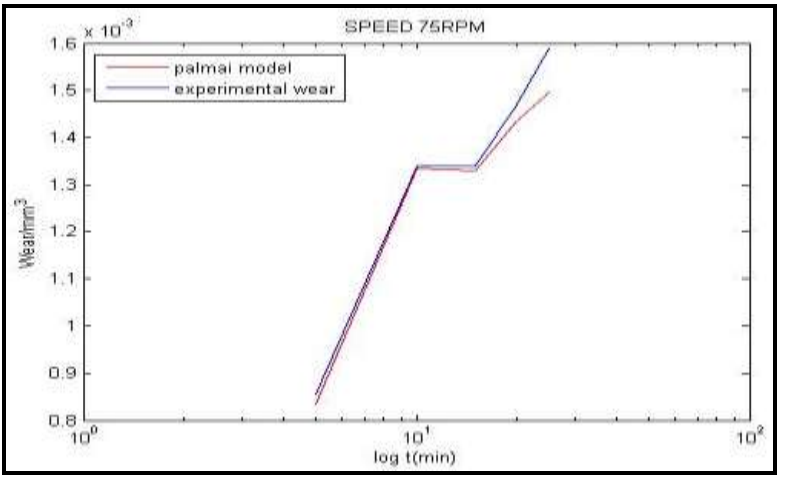


Fig. 18 Comparison of Experimental and Palmai wear for High Speed Tool Steel on Bright Mild Steel

The Palmai model constants were calibrated using the experimental data for the high speed tool bright mild steel pair. From Fig. 18, the Palmai flank wear and experimental wear data clearly increases with cutting time. Both curves are in perfect correlation as can be seen in the wear profiles. Thus the experimental wear data clearly validates the Palmai flank wear model for this tool and work piece combination.

**Comparison of Experimental and Palmai wear for High Speed Steel Tool on Stainless Steel at 1mm depth of cut**

Fig. 19 shows the graph of experimental and Palmai wear against time for high speed steel cutting tool on stainless steel material at feed rate of 20.4mm/rev, spindle speed of 200rpm and depth of cut of 1mm.

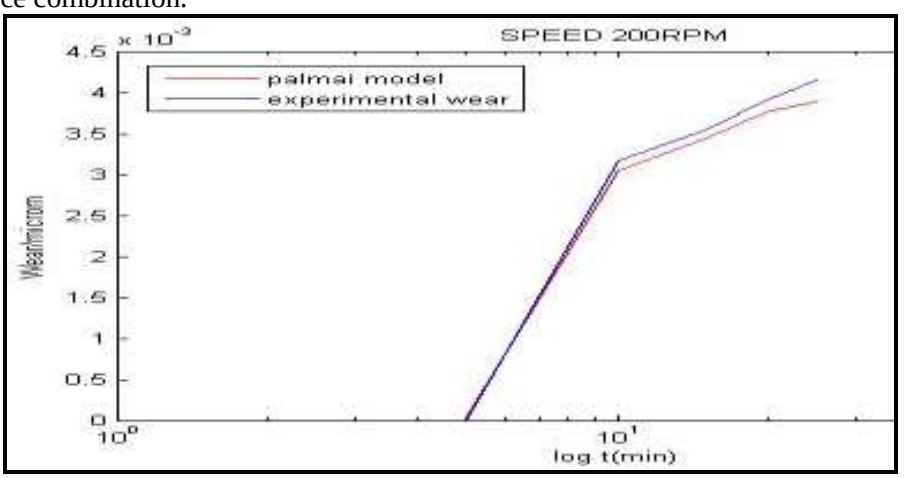


Fig. 19 Experimental and Palmai wear for High Speed Steel tool on Stainless Steel at 200rpm

The Palmai model constants were calibrated using the experimental data for the high speed steel and stainless steel pair. From Fig. 19 the Palmai flank wear and experimental wear

data clearly increases with cutting time.

Both curves are in perfect correlation as can be seen in the wear profiles. Thus the experimental wear data clearly validates the Palmai flank wear model for this tool/ workpiece combination.

**Comparison of Experimental wear and Palmai wear for High Speed Steel tool on Stainless Steel at 2mm depth of cut.**

Fig. 20 shows the graph of experimental and Palmai wear against time for high speed steel cutting tool on bright mild steel material at feed rate of 18.4mm/rev, spindle speed of 200rpm and depth of cut of 2mm.

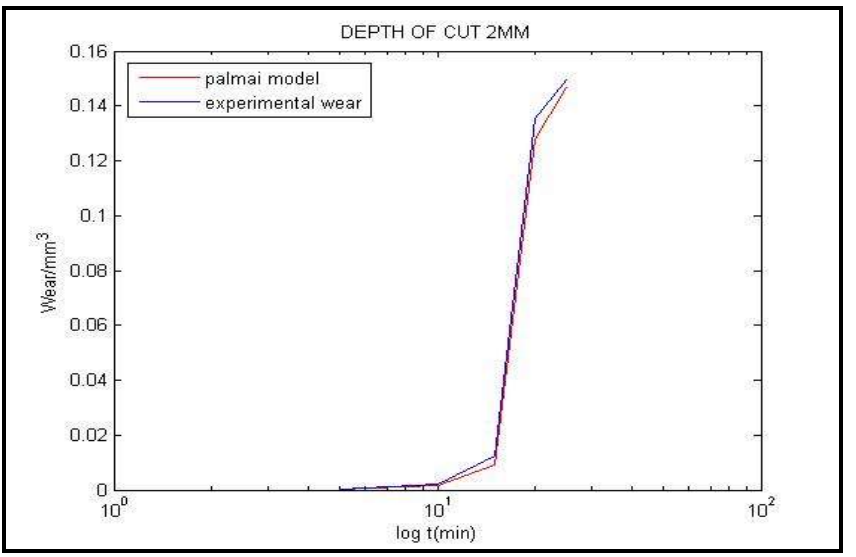


Fig. 20: Experimental and Palmai wear for high speed steel tool on stainless steel at 200rpm at 2mm depth of cut

The Palmai model constants were calibrated using the experimental data for the high speed steel and stainless steel pair. From Fig. 20 the flank wears and experimental wear data clearly increases with cutting time. Both curves are in perfect correlation as can be seen in the wear profiles. Thus the experimental wear data clearly validates the Palmai flank wear model for this tool and work piece combination.

## V. Conclusion

In this research, flank wear is analyzed using Palmai's model to determine the optimum cutting condition that will increase tool usage, thereby reducing production down time. This was achieved by conducting an experiment using two turning tools, High Speed Steel and ISOP 30 Carbide tools and two work piece materials Bright Mild Steel and Stainless steel on the Sumore SP 2110 lathe. The temperature of the tool was recorded using an infrared thermometer. The constants in the Paimai model were obtained numerically with the aid of 'fsolve' function of Matlab. The cutting parameters such as feed rate, depth of

cut and cutting speed played significant roles on tool wear. A result clearly shows that wear increased at higher speeds and depth of cut. Experimental and Paimai wear results show good correlation, with about 1.5% to 5.4% deviation.

**References**

[1] Senthilkumar, N., Tamizharasan, T. (2014), "Experimental investigation of cutting zone temperature and flank wear correlation in turning AIS11045 steel with different tool geometries", Indian Journal of Engineering and Material Science, Vol. 21, pp.139-148.

[2] Okonkwo, U. C., Okokpujie, I. P., Sinebe, J. E., and Ezugwu, C. A. (2015). Comparative analysis of aluminium surface roughness in end-milling under dry and minimum quantity lubrication (MQL) conditions. *Manufacturing Review*, *2*, 30.

[3]Okokpujie, Imhade P. and Okonkwo, Ugochukwu C. (2015) *Effects of Cutting Parameters on Surface Roughness during End Milling of Aluminium under Minimum Quantity Lubrication (MQL).* International Journal of Science and Research, 4 (5). pp. 2937-2942. ISSN 2319-7064

[4] Afolalu, Sunday A., Enesi Y. Salawu, Imhade P. Okokpujie, Abiodun A. Abioye, Oluwabunmi P. Abioye, Mfon O. Udo, Olajide R. Adetunji, and Omolayo M. Ikumapayi. "Experimental Analysis of the Wear Properties of Carburized HSS (ASTM A600) Cutting Tool." *International Journal of Applied Engineering Research* 12, no. 19 (2017): 8995- 9003.

[5] Okokpujie Imhade. P, Okonkwo Ugochukwu .C, Okwudibe Chinenye. D., "Cutting Parameters Effects on Surface Roughness During End Milling of Aluminium 6061 Alloy Under Dry Machining Operation", *International Journal of Science and Research (IJSR)*, www.ijsr.net, Volume 4 Issue 7, July 2015, 2030 – 2036

[6] Limbasiya G. (2011) "Seminar report on Tool Wear" Nirma University of diploma studies, India, pp. 17

[7] Nwoke, O. N., Okonkwo, U. C., Okafor, C. E., and Okokpujie, I. P. (2017). Evaluation Of Chatter Vibration Frequency in CNC Turning Of 4340 Alloy Steel Material. *International Journal of Scientific & Engineering Research*, *8*(2), 487-495.

[8] Janne L. (2008) "Visual measurement and modeling of tool wear in rough turning" Master thesis, Lappeenranta University of Technology

[9] Astakhov V. P. (2006) "Effects of the cutting feed, depth of cut, and workpiece (bore) diameter on the tool wear rate", The International Journal of Advanced Manufacturing Technology, Vol.34, pp.631-640.

[10]Astakhov V. P. (2006) "Tribology of Metal Cutting" Tribology and Interface Engineering Series, Elsevier vol. 52.

[11] Bjurka E. (2011) "Analysis of insert geometries, wear types and insert life in milling" Master's thesis in applied mechanics program, Chalmers University of Technology Goteborg Sweden pp. 9

[12]Groover, M.P.(2010) "Fundamentals of modern manufacturing", John-Wiley and sons, Inc, Hoboken, Chapter 21, pp.484-496.

[13] Coromant S. (1994) "Modern metal Cutting", Sandolken Sweden

[14] Palmai Z., Takac S. M., Farkas B. Z. (2013), 'Validation of new mathematical model of flank wear by different methods', materials science forum, Vol. 729, pp.169-174.

[15] Palmai, Z. (2014), 'A New physically defined equation to describe the wear of cutting tools', International Journal of Engineering,ISSN: 1584-2673.

[16] Imhade Princess Okokpujie, Omolayo M. Ikumapayi, Ugochukwu C. Okonkwo, Enesi Y. Salawu, Sunday A. Afolalu, Joseph O. Dirisu, Obinna N. Nwoke, and Oluseyi O. Ajayi (2017). Experimental and Mathematical Modeling for Prediction of Tool Wear on the Machining of Aluminium 6061 Alloy by High Speed Steel Tools. Open Eng. 7, 1–9

[17] Pálmai, Z. (2013), Proposal for a new theoretical model of the cutting tools flank wear. Wear pp. 291-222.

[18]Senthilkumar K. S., Senthilkumar J. S. (2014) "Analysis of flank Morphology when machining super duplex stainless steel in a gas cooled environment" International Journal of Engineering Technology, vol. 5 pp. 5047-5049.